

Quantitative Assessment of Artery Motion Compensation in IVUS Sequences

Aura Hernández¹, Oriol Rodríguez² and Debora Gil¹

¹ *Computer Vision Center and Computer Science Department, UAB, Bellaterra, Spain*

² *Hospital Universitari Germans Trias i Pujol, Badalona, Spain*

E-mail: aura, debora@cvc.uab.es

Abstract Cardiac dynamics suppression in IVUS is a main issue for visual improvement and extraction of tissue biomechanics in IntraVascular Ultra-Sound (IVUS). Although in recent times several motion compensation techniques have arisen, there is a lack of objective evaluation of motion reduction in *in vivo* pullbacks. We consider that the assessment protocol deserves special attention for the sake of a clinical applicability as reliable as possible. Our work focuses on defining a quality measure and a validation protocol assessing IVUS motion compensation. Synthetic experiments validate the proposed score as measure of motion parameters accuracy; while results in *in vivo* pullbacks show its reliability in clinical cases.

Keywords: validation standards, IVUS motion compensation, conservation laws.

1 Introduction

Assessment of tissue biomechanical properties (like strain and stress) are playing an increasing role in diagnosis and long-term treatment of intravascular coronary diseases [1, 2]. Arterial tissue elastic properties, and detection of rupture-prone vulnerable plaques, in particular, are one of the most active areas of research in both the cardiology and biomedical imaging communities [1, 2, 3, 4]. Determination of the main mechanical properties, currently under study, requires exploring vessel tissue deformation along the cardiac cycle. By their capability of reflecting vessel morphology and dynamics, IntraVascular UltraSound sequences represent a useful tool for the evaluation of tissue mechanical properties. However, cardiac dynamics introduce a misalignment of vessel structures in images as well as a saw-tooth-

shape in the longitudinal view appearance of vessel borders that hinders visualization, accuracy of volumetric measures and evaluation of tissue deformation [5]. This has motivated, in the last years, the development of several IVUS in-plane motion compensation techniques [6, 7, 8, 9].

In order to ensure a high applicability in clinical practice, special care should be taken in defining an objective measure allowing assessment of motion parameters accuracy in real data. In real pullbacks there is no objective error measure indicating the amount of motion suppressed, since motion parameters are unknown. In most cases, quality measures are either subjective measures, based on the visual appearance of sequences and longitudinal cuts [6], [9] or rely on extraction of vessel properties (such as strain in [7]). We consider that such an important issue as the validation protocol deserves special attention.

This paper addresses the definition of assessment standards for the objective measure of rigid motion reduction in IVUS sequences. We approach defining a quantitative score of dynamics compensation, as well as, provide an experimental setting for its validation for clinical practice. Our score bases on the grounds of fluid mechanics conservation laws [10] and considers the changes that the local density of mass (given by the image local mean) experiences along the sequence. The comparison of the former quantity before and after motion correction defines our quality measure, which we call Conservation of Density Rate (*CDR*). Regarding the experimental setting, two sets of experiments are presented: validation of motion assessment on phantom sequences and performance in real pullbacks. Synthetic experiments explore the ability of *CDR* to quantify the rate of image alignment. Results on *in vivo* pullbacks

show *CDR* correlation to visual appearance of longitudinal cuts.

The remains of the paper are structured as follows. Section 2 is devoted to the definition of the quality measure. Experiments on phantom and real sequences are reported in Section 3. Discussions and conclusions are detailed in Section 4.

2 Assessment of Cardiac Rigid Motion Compensation

Any comparative quantity reflecting image changes along a sequence, captures, in the case of IVUS, differences in morphology as well as vessel misalignments. After motion correction, vessel displacement has disappeared, but morphological changes still remain. Therefore, even in the best case, comparison of aligned images along the sequence is prone to give a non-constant function depending on the particular morpho-geometric changes of the vessel segment. We conclude that in order to properly quantify vessel alignment, only the dynamic components should be taken into account.

Since vessel dynamics is mainly induced by cardiac motion, we use the Fourier transform for comparing cardiac terms. Let $\widehat{CQ}_0, \widehat{CQ}_1$ be the Fourier developments of any comparative quantity before and after motion correction, and consider the principal cardiac frequency, namely ω_c . We define the Cardiac Alignment Rate (*CAR*) as:

$$CAR := 1 - \frac{A_{\widehat{CQ}_1}(\omega_c)}{A_{\widehat{CQ}_0}(\omega_c)}$$

for $A_{\widehat{CQ}_0}(\omega_c)$ and $A_{\widehat{CQ}_1}(\omega_c)$ the amplitudes corresponding to the cardiac frequency of \widehat{CQ}_0 and \widehat{CQ}_1 , respectively. The *CAR* index equals 1 in the case that all cardiac motion has been suppressed, while approaches zero (or becomes even negative) for a poor rate of motion reduction.

Concerning the comparative quantity, in most cases it relies on a similarity measure between images, since the value obtained by comparing each frame to a reference frame reflects differences along the sequence. Unfortunately, usual similarity measures (like Mutual Information (MI) [11] or Cross Correlation [12]) are sensitive to texture, speckled noise and uniform grey-value areas and, thus, are

prone to miss estimate the amount of alignment [13]. Figure 1 illustrates this phenomenon in the case of mutual information. Images on the first two columns correspond to two frames captured at different times for the original sequence and the corrected one. Images on the last column correspond to the absolute value of the difference between the two frames and illustrate the amount of motion between them. The plot on the right represents the joint distribution for the image grey-values. For each image pixel, its grey-value on each of the two frames captured at different times provides its x - y coordinates on the plot. Black points correspond to the original sequence and light crosses to the corrected one. Although the misalignment between original images has been properly compensated, both point clouds present a comparable scatter and thus their MI will be similar.

Vessel motion is not visually noticed at all image pixels but only at some salient areas, such as calcium transitions or adventitia points of extreme curvature. This motivates adopting a local approach and tracking image motion for each pixel. Usual similarity measures compare images in the framework of integrable functions [14] and are prone to give less reliable outputs if they are computed on small sets of pixels. Inspired on the strategies used in classic fluid mechanics [10], we propose exploring the conservation of a physical quantity along the sequence. In particular, we have chosen the local density of mass, since it will remain constant along the sequence in the measure that vessel structures are aligned. By the ultrasound properties, the image grey-values are proportional to the density of mass of tissue. We approximate the tissue local density by the image local mean computed in sliding windows 9×9 pixels large. The values of the local mean for all images provide each pixel with a function that describes the conservation of the local density of mass along the sequence. The *CAR* score for each of these functions provides a measure of the amount of local motion around each pixel.

Figure 2 sketches the main steps involved in the computation of our quality measure: computation of the image descriptor (upper block), conservation of local density along the sequence for a given pixel (middle block) and the *CAR* value for all pixels (bottom block). The first block illustrates the modeling of the local density of mass in terms of the image local mean. The local mean of the image (shown on

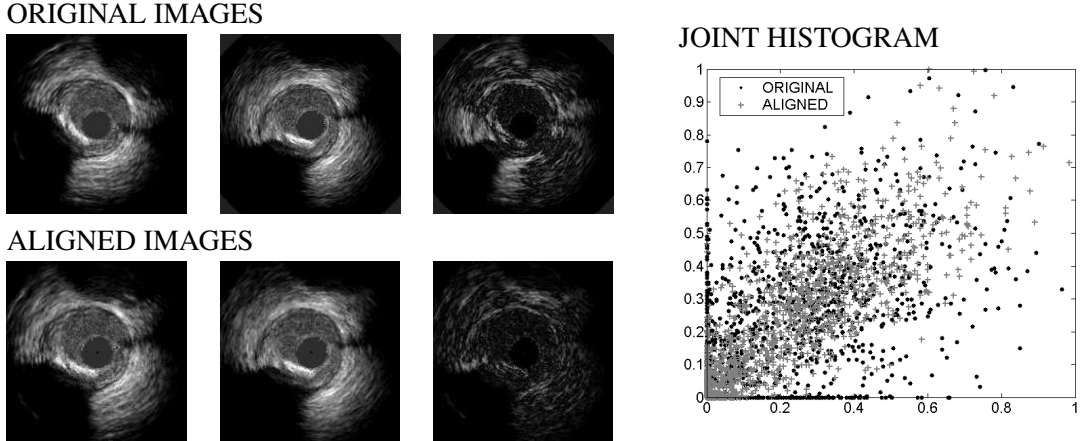


Figure 1: Limitations of similarity measures (e.g, mutual information) for image alignment quantification.

the right) is obtained by computing, for each pixel, the image mean on a window (white square on the left image) centered on each pixel (black point). In the second block of the figure, we have the evolution of the local mean at a single pixel before (plot on the left) and after (plot on the right) image alignment. The plot obtained before alignment presents a well defined periodic behavior; afterwards, although the periodic pattern has been suppressed, the function still presents a variability due to noise and morphologic changes. The third block shows the *CAR* values obtained for all image pixels. The top plot shows the sorted *CAR* values and the bottom images show the position on the image of pixels achieving extreme values (dotted squares on the *CAR* plot). Since rigid motion is a global movement, all pixels in an image should present a similar *CAR* value. However, at blood and outer areas (not belonging to vessel structures) *CAR* achieves extreme low values (left bottom image), because motion is not noticeable. Meanwhile, pixels showing motion (like the calcium tissue transition on the right image) present a uniform (high) *CAR* value. In fact, the sorted *CAR* values (top plot) asymptotically converge towards the true motion reduction rate. It follows that only *CAR* upper percentiles properly contribute to the amount of motion reduced.

We define our Conservation of Density Rate (*CDR*) as the trimmed mean [15] of the *CAR* value computed for the image local average:

$$CDR := \mu(\{CAR \mid CAR > prct\}) \quad (1)$$

for *prct* a given percentile. The *CDR* score, as well as any error, can be regarded as a random variable. In

this framework, we have empirically proved (see experiments on phantoms in sect. 3.1) that the *CDR* computed for the superior 66% percentile statistically correlates to the rotation angle relative error.

3 CDR Validation

3.1 Phantom Data

Our synthetic experiments focus on addressing the reliability of *CDR* as measure of motion compensation. Phantoms have been generated by applying a motion pattern to a block of IVUS images representing a still artery pullback. Motion patterns have been extracted from parameters estimated from 5 test sequences. The algorithm used to compute IVUS motion is the one described in [8], which considers compensation of in-plane rigid motion. Regarding image sequences two different phantoms have been considered: a Static model based on a unique image block and a Sequence-based model obtained by compensating motion of an *in vivo* pullback. The latter do not belong to the set of sequences used for extracting the motion patterns.

Absolute and relative differences between true motion parameters and estimated ones provide, for each sequence, an error function. The average ($\|\cdot\|_1$ norm) of the error function is our quality measure for each phantom and its statistical range (given by the mean \pm the variance) reports the performance for all cases. In order to validate the quality measure we have compared *CDR* values to the relative accuracy (in percentage) given by 1 minus the relative error.

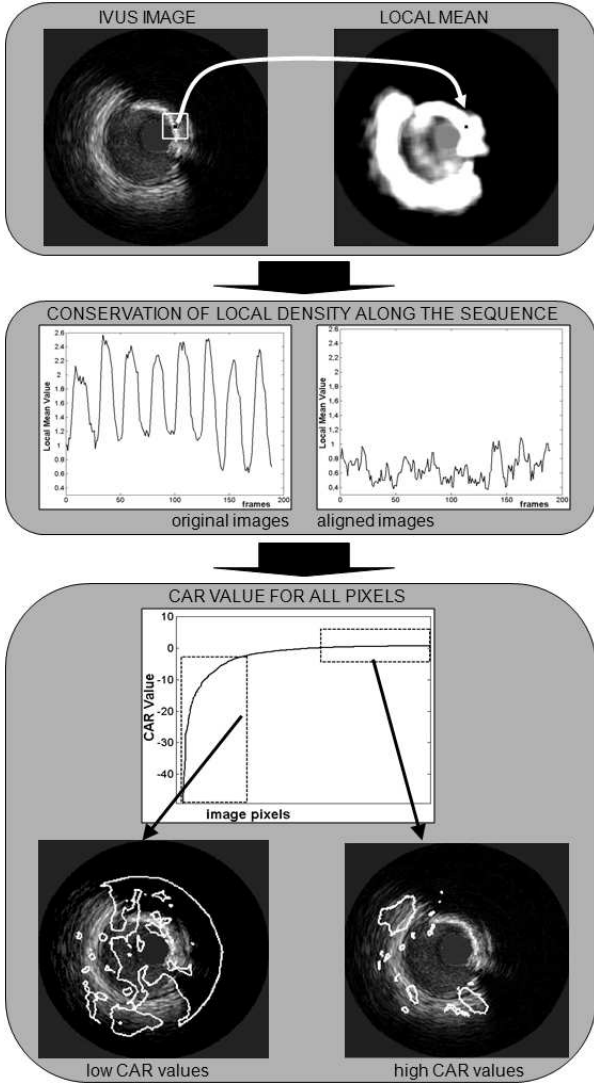


Figure 2: Quality Measure Computation

We have chosen the angle relative accuracy since its computation [8] depends on the center of mass and, thus, it reflects the overall error. Student T-tests and confidence intervals (at 95% of confidence) are used to check whether there is any significant difference between means.

Table 1: *CDR* Correlation to Motion Compensation

	Static	Sequence
ABS. ACC.	0.32 ± 0.15	2.19 ± 1.19
REL. ACC.	95.23 ± 4.39	75.13 ± 12.94
<i>CDR</i>	93.25 ± 4.67	78.40 ± 7.43
p-val	0.1800	0.8530
CI	(-0.98, 4.93)	(-7.16, 5.99)

Table 1 reports the statistics summary for the validation of *CDR* (computed on the upper 66% *CAR* percentile) as accuracy score. We report, for both phantoms, ranges for the angle absolute accuracy (ABS. ACC.), the angle relative accuracy (REL. ACC.) and *CDR*, as well as, the T-test p-value and the confidence interval (CI) for the difference in means. There is no significance difference between *CDR* and relative accuracy with at most a discrepancy between -7.16% and 5.99% .

3.2 Experimental Data

Performance in real pullbacks has been validated by testing the proposed approach in 32 vessel segments extracted from clinical cases of the Hospital Universitari "Germans Trias i Pujol" in Badalona, Spain. Sequences have been recorded using a Galaxy-BostonSci device at 40 MHz, constant pull-back and a digitalization rate of 30 fps. The segments analyzed are short segments 5-6 mm long and cover different plaques (from soft to calcified), morphologies (including branches) and motion artifacts (such as longitudinal motion). Motion was compensated using the approach to rigid movement described in [8].

Figure 3 shows four cases with decreasing *CDR* values (from left to right): 87%, 81%, 78% and 60%. The first row shows a frame of the original sequences, the second one the longitudinal cuts before motion compensation and the last row the cut after sequence alignment. In the first column (fig.3(a)) we show a sequence with structure misalignment. The calcium shadow appears and disappears in the original longitudinal cut due to rotation, while calcium presents a uniform appearance in the aligned cut. In the second column (fig.3(b)) we show a sequence presenting a noticeable vessel translation and its associated tooth-saw-shape in the original longitudinal cut (especially at the end of the segment). After motion correction, only a subtle undulation due to radial dilation (at the beginning of the cut) remains. The longitudinal cuts in fig.3(c) show a straight profile (both before and after alignment) in spite of a lower *CDR*. This phenomenon, which appears in the absence of motion, is inherent to any relative measure (like *CDR* and is discussed in detail in section 4. Finally, in fig.3(d) we show the worst performer both in terms of longitudinal cut appearance and *CDR* value.

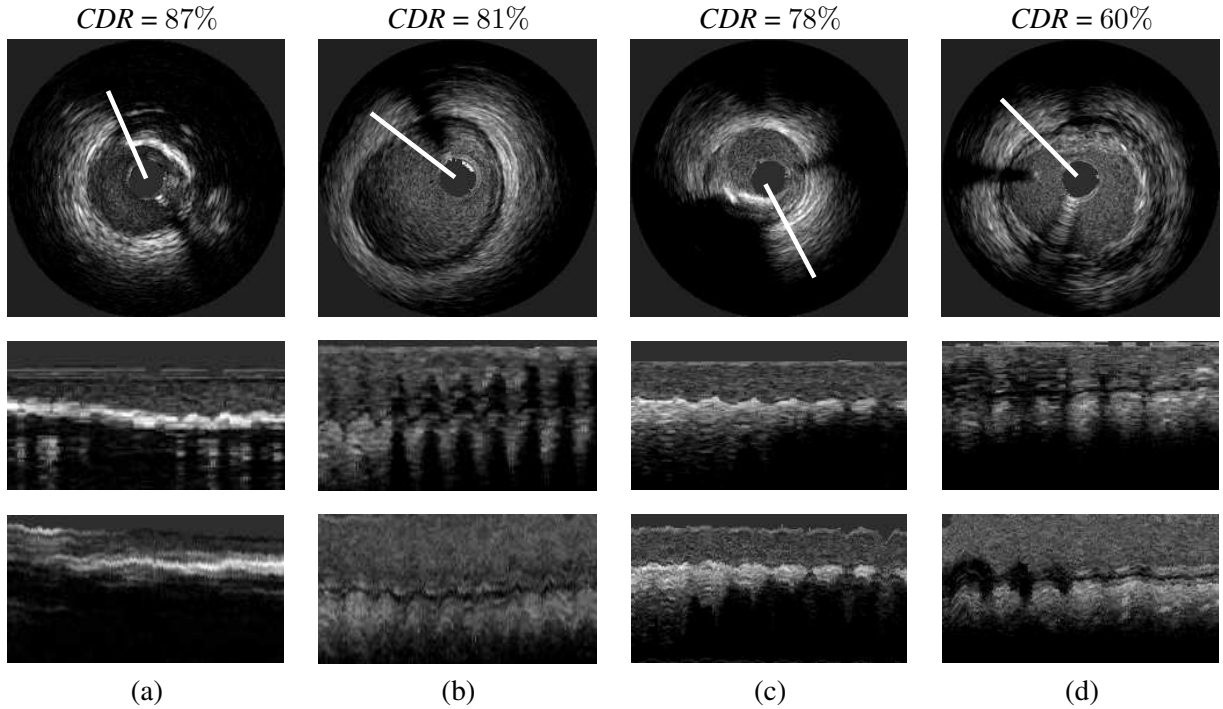


Figure 3: Longitudinal cuts. Each column corresponds to each patient, from the best CDR to the worst one.

In this last case, a proper alignment is only achieved at the second half of the segment and, those, we have only a 60% of motion reduction.

3.3 Clinical Potential

A potential application of the method for clinical practice is tracking of continuous structures difficult to segment in original sequences. Stabilized sequences preserve local density of mass of structures along the time, so a mean of the sequence enhances those structures, while blurs texture and speckle.

Figure 4 shows a simple example of the continuity of the stabilized structures. We have computed edges on average of stabilized and non-stabilized sequences. The CDR compensation rate was 84%. Sobel edges are shown on the first column and Canny on the second one. The first row shows the output for the original sequence, while edges computed on the stabilized sequences are shown on the second one. We note that, after a high CDR reduction, both Canny and Sobel give continuous profiles of the vessel external wall.

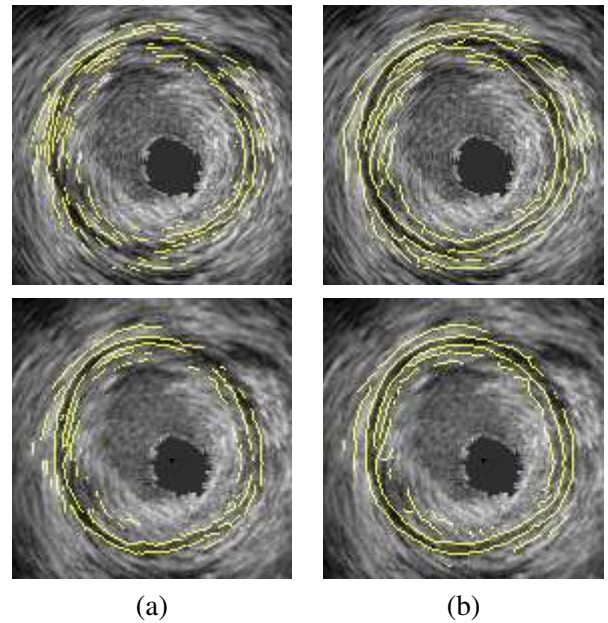


Figure 4: Sobel (left) and Canny (right) edge detectors to a mean of the sequence before (upper) and after (down) the alignment.

4 Discussion and Conclusions

This paper approaches assessment of artery motion compensation in IVUS sequences. We address the

definition of an objective score (*CDR*) measuring motion reduction in experimental data. We present experiments on synthetic sequences (phantoms) and *in vivo* pullbacks and also a clinical application.

Performance on phantoms sequences (table 1) shows that *CDR* statistically compares to the relative accuracy in parameter estimation, which validates it as a motion suppression measure. Results on real pullbacks show that, in general, *CDR* also correlates to the appearance of longitudinal cuts (see figure 3(a), (b) and (d)). There are only two cases which *CDR* values are not as high as expected. On one side, real sequences present both rigid and non-rigid motion, although only the rigid component is suppressed. As a result, *CDR* under estimates motion reduction in experimental data presenting radial dilation, like the case in fig.3(b). On the other side, for those sequences with little motion (see fig.3(c)), *CDR* does not fit either longitudinal cut visual appearance or absolute accuracy. This follows, because it is a relative score and we recall that, in the case of low motion, only sub-pixel accuracy (unfeasible to achieve) guarantees a high *CDR* score.

By the former considerations we conclude that the *CDR* score is an objective measure of image alignment in experimental data which correlates to parameters accuracy and longitudinal cuts appearance. The fact that its computation relies exclusively on image local appearance evolution validates the *CDR* score as experimental measure of image alignment. Its clinical usefulness is shown by improving the detection and tracking of vessel structures (e.g, external wall).

Acknowledgment

This work was supported by the Spanish Government FIS projects PI070454 and PI071188. The last author is supported by The Ramón y Cajal Program.

References

- [1] Wentzel, J., et al, R.K.: Relationship between neointimal thickness and shear stress after wallstent implantation in human coronary arteries. *Circulation* **103**(13) (2001) 1740–5
- [2] Garcia, J., Crespo, A., Goicolea, J., Sanmartin, M., Garcia, C.: Study of the evolution of the shear stress on the restenosis after coronary angioplasty. *Journal of Biomechanics* **39**(5) (2006) 799–805
- [3] Kakadiaris, I.A., O'Malley, S.M., Vavuranakis, M., Carlier, S., Metcalfe, R., Hartley, C.J., Falk, E., Naghavi, M.: Signal-processing approaches to risk assessment in coronary artery disease. Technical Report UH-CS-06-09, Department of Computer Science, University of Houston (June 2006)
- [4] Céspedes, E., Korte, C., van der Steen, A.: Intraluminal ultrasonic palpation: assessment of local cross-sectional tissue stiffness. *Ultrasound Med. Biol.* **26** (March 2000) 385–396
- [5] Delachartre, P., Cachard, C., Finet, G., Gerfault, F., D.Vray: Modeling geometric artefacts in intravascular ultrasound imaging. *Ultrasound Med Biol* **25**(4) (1999) 567–575
- [6] de Winter, S.A., Hamers, R., Degertekin, M., et al.: Retrospective image-based gating of intracoronary ultrasound images for improved quantitative analysis: The intelligate method. *Catheterization and Cardiovascular Interv* **61** (2004) 84–94
- [7] Leung, K.Y.E., Baldewsing, R., Mastik, F., et al.: Motion compensation for intravascular ultrasound palpography for in vivo vulnerable plaque detection. In: *IEEE Ultrasonics Symposium*. Volume 1. (2005) 253–256
- [8] Hernández, A., Radeva, P., Tovar, A., Gil, D.: Vessel structures alignment by spectral analysis of ivus sequences. In: *Proc. of CVII, MICCAI Workshop*. (2006)
- [9] Rosales, M., Radeva, P., Rodriguez, O., Gil, D.: Suppression of IVUS image rotation. a kinematic approach. In: *FIMH*. Volume 3504. (2005) 359–368
- [10] Whitaker, S.: *Introduction to Fluid Mechanics*. Krieger Pub Co (1992)
- [11] Viola, P., Wells, W.: Alignment by maximization of mutual information. *Journal of Computer Vision* **24** (1997) 137–154
- [12] Pratt, W.: *Digital Image Processing*. 2nd edn. Wiley, New York (1991)
- [13] Pluim, J.P.W., Maintz, J.B.A., Viergever, M.A.: Mutual information based registration of medical images: a survey. *IEEE Trans. Med. Imag.* **22**(8) (2003) 986–1004
- [14] Rudin, W.: *Complex and Real Analysis*. McGraw-Hill Int. Ed. (1987)
- [15] Rousseeuw, P., Leroy, A.: *Robust Regression and Outlier Detection*. John Wiley and Sons (1987)